Journal of Neurocytology **28**, 169–185 (1999)

Immunocytochemical localization of D-amino acid oxidase in rat brain

SANDRA MORENO[1*], ROBERTA NARDACCI[2], ANNAMARIA CIMINI[3] and MARIA PAOLA CERÙ[3]

[1] *Dipartimento di Biologia, Università Roma Tre, Roma 00146, Italy;* [2] *Dipartimento di Biologia Cellulare e dello Sviluppo, Università di Roma La Sapienza, Roma 00185, Italy;* [3] *Dipartimento di Biologia di Base ed Applicata, Università dell'Aquila, Coppito 67010 L'Aquila, Italy*

Received 18 August 1998; revised 7 January and 14 May 1999; accepted 21 May 1999

Summary

D-amino acid oxidase (D-AAO) is a peroxisomal flavoenzyme, the physiological substrate and the precise function of which are still unclear. We have investigated D-AAO distribution in rat brain, by immunocytochemistry, with an affinity-purified polyclonal antibody. Immunoreactivity occurred in both neuronal and glial cells, albeit at different densities. Glial immunostaning was strongest in the caudal brainstem and cerebellar cortex, particularly in astrocytes, Golgi-Bergmann glia, and tanycytes. Hindbrain neurons were generally more immunoreactive than those in the forebrain. Immunopositive forebrain cell populations included mitral cells in the olfactory bulb, cortical and hippocampal neurons, ventral pallidum, and septal, reticular thalamic, and paraventricular hypothalamic nuclei. Within the positive regions, not all the neuronal populations were equally immunoreactive; for example, in the thalamus, only the reticular and anterodorsal nuclei showed intense labelling. In the hindbrain, immunopositivity was virtually ubiquitous, and was especially strong in the reticular formation, pontine, ventral and dorsal cochlear, vestibular, cranial motor nuclei, deep cerebellar nuclei, and the cerebellar cortex, especially in Golgi and Purkinje cells.

Introduction

D-amino acid oxidase (D-AAO) is a flavoenzyme first characterized in the early 1930s, that catalyzes the oxidative deamination of D-amino acids (Krebs, 1935). This enzyme is widely present in prokaryotes and eukaryotes, including mammals, where it is mainly localized in the kidney and liver. Although many studies *in vitro* have led to detailed clarification of the structure, amino acid sequence, substrate specificity (also in relation to different species), and kinetic mechanism of D-AAO (Dixon & Kleppe, 1965; Bright & Porter, 1975; Ronchi *et al.*, 1982; Konno *et al.*, 1982; D'Aniello *et al.*, 1993a), the function of this enzyme *in vivo* remains obscure, as its physiological substrate is still unknown. In fact, in higher animals, D-amino acids were believed to be present only in trace amounts. This raised the possibility that the natural substrate might not be D-amino acids (Hamilton, 1985). However, several lines of evidence obtained by using mutant mice lacking D-AAO (Konno & Yasumura, 1983), suggest that the enzyme might be involved in neutral D-amino acid metabolism (Konno & Yasumura, 1992). Moreover, the administration of free D-amino acids to pregnant and lactating rats induces a specific increase of liver and kidney D-AAO in their offspring (D'Aniello *et al.*, 1993).

Recently, considerable concentration of endogenous D-serine has been detected in mouse and rat brain (Nagata, 1992; Hashimoto *et al.*, 1992) and an inverse correlation between the amount of this D-amino acid and D-AAO activity has been shown in various regions, at different developmental ages (Horiike *et al.*, 1994; Nagata *et al.*, 1994; Hashimoto *et al.*, 1995; Schell *et al.*, 1995). These observations led to the proposal that the oxidase in the brain may specifically deaminate D-serine, which is supposed to act as a neuromodulator, by activating the N-methyl-D-aspartate (NMDA) receptor complex, through binding to the strychnine-insensitive glycine-binding site (Hashimoto *et al.*, 1993; Fedele *et al.*, 1997).

D-AAO is localized in peroxisomes, ubiquitous cytoplasmic organelles involved in a number of anabolic and catabolic processes, such as acyl-CoA ß-oxidation,

* To whom correspondence should be addressed.

0300–4864

biosynthesis of plasmalogens, bile acids, cholesterol and dolichol, amino acid metabolism, glyoxilate metabolism and catabolism of purines, phytanate and pipecolate (Van den Bosch *et al.*, 1992). While the distribution, morphological features, protein composition, and functions of peroxisomes have been extensively investigated in liver and kidney, their precise role in nervous tissue is still unclear, as they are especially difficult to study due to their relative paucity and small size (Holtzman, 1982). Important functions of peroxisomes in the CNS are suggested by the existence of congenital peroxisomal diseases, most of which involve severe neurological disorders, originating by both developmental and degenerative disturbances (Moser, 1987).

A complete map of the distribution in the rat CNS of catalase, considered as a peroxisomal marker enzyme, was previously obtained by our group. This was achieved by immunocytochemistry utilizing an extremely sensitive intensification procedure based on the deposition of biotinylated tyramine on the tissue, through the action of peroxidase (Adams, 1992; Moreno *et al.*, 1995). We reported the presence of catalase immunoreactivity both in neuronal and glial cells, albeit at different densities in different brain regions and in different cell types.

In the CNS, D-AAO localization has been investigated by means of cytochemical methods, based on the ability of D-AAO-produced H_2O_2 either to directly oxidize cerium ions (Arnold *et al.*, 1979) or to peroxidize 3,3′-diaminobenzidine in a coupled peroxidase catalyzed reaction (Horiike *et al.*, 1987, 1994). These reports agree in finding enzymatic activity in astrocytes, but not in other glial cell types or neurons. Moreover, a regional inhomogeneity in D-AAO distribution and, specifically, its abundance in the cerebellum and brainstem, as compared to the forebrain, was described (Horiike *et al.*, 1994).

To date, immunocytochemical methods have been successfully applied to investigate D-AAO localization in kidney and liver, also at the ultrastructural level (Usuda *et al.*, 1986, 1991; Perotti *et al.*, 1987). However, to our knowledge, the only paper dealing with the immunolocalization of D-AAO in nervous tissue describes the immunofluorescence pattern in the cerebellum (Weimar & Neims, 1977).

The aim of our study was to investigate the immunocytochemical distribution of D-AAO in rat brain, revealed by means of the tyramine intensification method (Adams, 1992), using an affinity-purified polyclonal antibody prepared in our laboratory (Cimini *et al.*, 1998). The specificity of the antibody was assayed both by immunoblotting and by immunoelectron microscopy on rat kidney and brain.

Materials and methods

ANTIBODY

Polyclonal antiserum was raised in rabbit, using conventional procedures, against hog kidney D-AAO (Sigma, St. Louis, MO). The antiserum was affinity purified (Cimini *et al.*, 1998) and its specificity was tested by immunoblotting.

IMMUNOBLOTTING

Hog kidney D-AAO (20 ng), rat brain and liver total homogenate (50 and 25 μg, respectively) were resolved by SDS-PAGE on 10% polyacrylamide gel according to Laemmli (1979). The following prestained proteins (Sigma) were used as molecular weight (Mr) standards: β-galactosidase (116 000), fructose-6-phosphate kinase (84 000), pyruvate kinase (58 000), lactic dehydrogenase (36 500), trypsin inhibitor (20 100), α-lactalbumin (14 200). Proteins were then electrically transferred onto nitrocellulose sheet (0.45 μm, Sigma) according to Towbin *et al.* (1979). Sheets were incubated with 3% BSA in PBS to block aspecific binding, overnight at 4°C, then with anti-D-AAO (1 : 500 in PBS containing 0.1% Tween 20) for 3 h at room temperature (RT), and finally with horseradish peroxidase (HRPO)-conjugated goat anti-rabbit antibody (Amersham, Buckinghamshire, UK) (1 : 3000 in PBS-Tween), for 1 h at RT. Immunoreactive bands were visualized by enhanced chemiluminescence (ECL Western blotting detection set, Amersham). Extensive washings with PBS-Tween were carried out between each step. Controls were performed on the same samples, by using the primary antibody after incubation with excess antigen (1 : 50) overnight at 4°C.

ANIMALS

Twelve adult Fischer rats of either sex, weighing about 250 g, kept on a standard laboratory diet and water *ad libitum*, were used for this study. All animals were housed and handled according to guidelines proposed by the Society for Neuroscience and the Italian National Research Council, and were deeply anesthetized with pentobarbital (40 mg/kg b.w., injected intraperitoneally) before rapid killing by transcardial perfusion with the fixative solution.

LIGHT MICROSCOPIC IMMUNOCYTOCHEMISTRY

Rats were perfused at room temperature with physiological saline followed by a zinc-formol fixative consisting of 4% commercial formaldehyde, 0.5% zinc salicylate and 0.9% NaCl, pH 6.2 (Mugnaini & Dahl, 1983). Other rats were perfused with a calcium-free Ringer's variant saturated to pH 7.3 with 95% O_2 and 5% CO_2, followed by 4% freshly depolymerized paraformaldehyde in 0.12 M phosphate buffer (PB), pH 7.3. The brains were removed one hour after perfusion and left 48 hours at 4°C in a cryoprotectant solution (30% sucrose in physiological saline). Serial, sagittal, or coronal brain sections were cut on a freezing stage microtome at 25 μm, and collected in phosphate buffered saline (PBS), pH 7.3. The free floating sections were incubated for 1 hour in 2% non-fat dry milk and 0.1% Triton-X

100, under gentle agitation. After rinsing in PBS, sections were incubated in the primary antibody diluted 1 : 600 in PBS containing 1% non-fat dry milk and 0.05% Triton-X 100 and then processed according to the amplification procedure of the avidin-biotin-HRPO system localized with DAB (Adams, 1992). Biotinylated secondary antiserum, normal goat serum, and avidin-biotin-HRPO (Standard ABC kit) were purchased from Vector (Burlingame, CA, USA); NHS-biotin from Pierce Chemical Co. (Rockford, IL, USA), tyramine and DAB (3,3′-diaminobenzidine) from Sigma. Each step was followed by extensive wash with PBS. The sections were mounted in 3 : 1 glycerol-0.4 M phosphate buffer, pH 7.4, and sealed with nail polish. For controls, (a) preimmune serum was substituted for the primary antiserum, or (b) the primary antiserum was pre-incubated with excess antigen, or (c) the primary antiserum was omitted. Control sections were free of immunoreaction product.

PRE-EMBEDDING IMMUNOELECTRON MICROSCOPY

Rats were perfused with a calcium-free Ringer's variant saturated to pH 7.3 with 95% O_2 and 5% CO_2, followed by 4% freshly depolymerized paraformaldehyde in 0.12 M PB, pH 7.3. One hour after perfusion, the brains were dissected out and cut coronally on a Vibratome at 30–40 μm. Sections were collected in PB and then transferred to PBS containing 2% non-fat dry milk and 0.1% Triton X-100 for 1 hour. Sections were incubated in the primary antibody diluted 1 : 600 in PBS containing 1% non-fat dry milk and 0.05% Triton-X 100 for 24 hours at 4°C, under gentle agitation, and finally they were processed as specified above. After the immunoreaction, slices were post-fixed in OsO_4 and uranyl acetate, dehydrated, flat-embedded in Epon, remounted on Epon blanks, and sectioned on an ultramicrotome. Ultra-thin sections were photographed in a Philips CM120 electron microscope.

POST-EMBEDDING IMMUNOELECTRON MICROSCOPY

Two rats were killed by decapitation and kidneys were quickly removed. Kidney cortices were cut in smaller pieces and immersed in 1% freshly depolymerized paraformaldehyde with 0.2% glutaraldehyde in 0.1 M cacodylate pH 7.4, containing 0.05% calcium chloride, for 1 hour at 4°C. Samples were rinsed in buffer, partially dehydrated (up to 95% alcohol), and embedded in London Resin White (LR White, Agar Scientific Ltd., Stanted, UK) at 4°C for 48 hours. Tissue blocks were cut on an ultramicrotome, and ultrathin sections were processed for immunogold technique. Grids were pre-incubated with 10% normal goat serum in 10 mM PBS containing 1% bovine serum albumin (BSA) and 0.13% NaN_3 (medium A), for 15 minutes at RT; sections were then incubated with primary antibody diluted 1 : 10 in medium A, overnight at 4°C. After rinsing in medium A containing 0.01% Tween 20 (Merck, Darmstadt, Germany), sections were incubated in goat anti-rabbit IgG conjugated to 15 nm colloidal gold (British BioCell Int., Cardiff, UK), diluted 1 : 20 in medium A containing fish gelatin, for 1 hour at RT. Grids were thoroughly rinsed in distilled water, contrasted with aqueous 2% uranyl acetate for 20 minutes, and photographed in a Philips CM120 electron microscope.

Results

SPECIFICITY OF THE ANTISERUM

The specificity of our affinity-purified anti-D-AAO antibody was tested by western blotting (Fig. 1A) and immunoelectron microscopy (Fig. 1B–D). Western blotting shows one band of about 40 kDa recognized by the anti-D-AAO antibody, when a suspension of purified hog kidney D-AAO is used (lane 1). One band of similar molecular weight is recognized also in brain and liver total homogenates (lanes 2 and 3, respectively). The specific D-AAO band is absent when the primary antibody is preadsorbed with the antigen (lanes 1′-3′). In the kidney cortex, D-AAO immunoreactivity revealed by post-embedding EM immunocytochemistry is exclusively localized to peroxisomes, and is especially high in proximal convoluted tubule epithelial cells (Zaar, 1992) (Fig. 1B). In the brain, D-AAO immunoreactivity revealed by pre-embedding EM immunocytochemistry is present both in neurons (Fig. 1C) and astrocytes (Fig. 1D). Reaction product is localized to cytoplasmic organelles morphologically recognizable as peroxisomes.

BRAIN

Comparable results were obtained with both fixation procedures used. D-AAO was detected in both neuronal and glial cells. Reaction product was confined to the cytoplasm of labelled cells, with a somewhat diffuse appearance. Immunoreactive cells were present to variable extents in both the forebrain and the hindbrain, as shown semi-quantitatively in Table 1 (nomenclature follows that of Paxinos & Watson, 1986).

NEURONS

In the rhinencephalon, the most intensely labelled elements are mitral cells of the olfactory bulb (Fig. 2A). Other positive cells include numerous medium to large neurons in the external plexiform layer, interpreted as tufted cells, and few medium-sized elements in the internal granular layer (Fig. 2A). Immunoreactive neurons are also found in layers 1a and 3 of the anterior olfactory nucleus (Fig. 2B). In the olfactory cortex, pyramidal cells of the piriform cortex and cells of the olfactory tubercle show distinct positivity (Figs. 2C and 3C).

The telencephalic cortex contains numerous strongly immunopositive neurons (Fig. 3A). Although regional differences are not marked, a slightly larger number of stained neurons is seen in the frontal area. The D-AAO positive neurons appear evenly distributed in the different layers. These include pyramidal cells, such as the giant neurons of layer V, and other cells with a distribution similar to GABAergic interneurons (Mugnaini

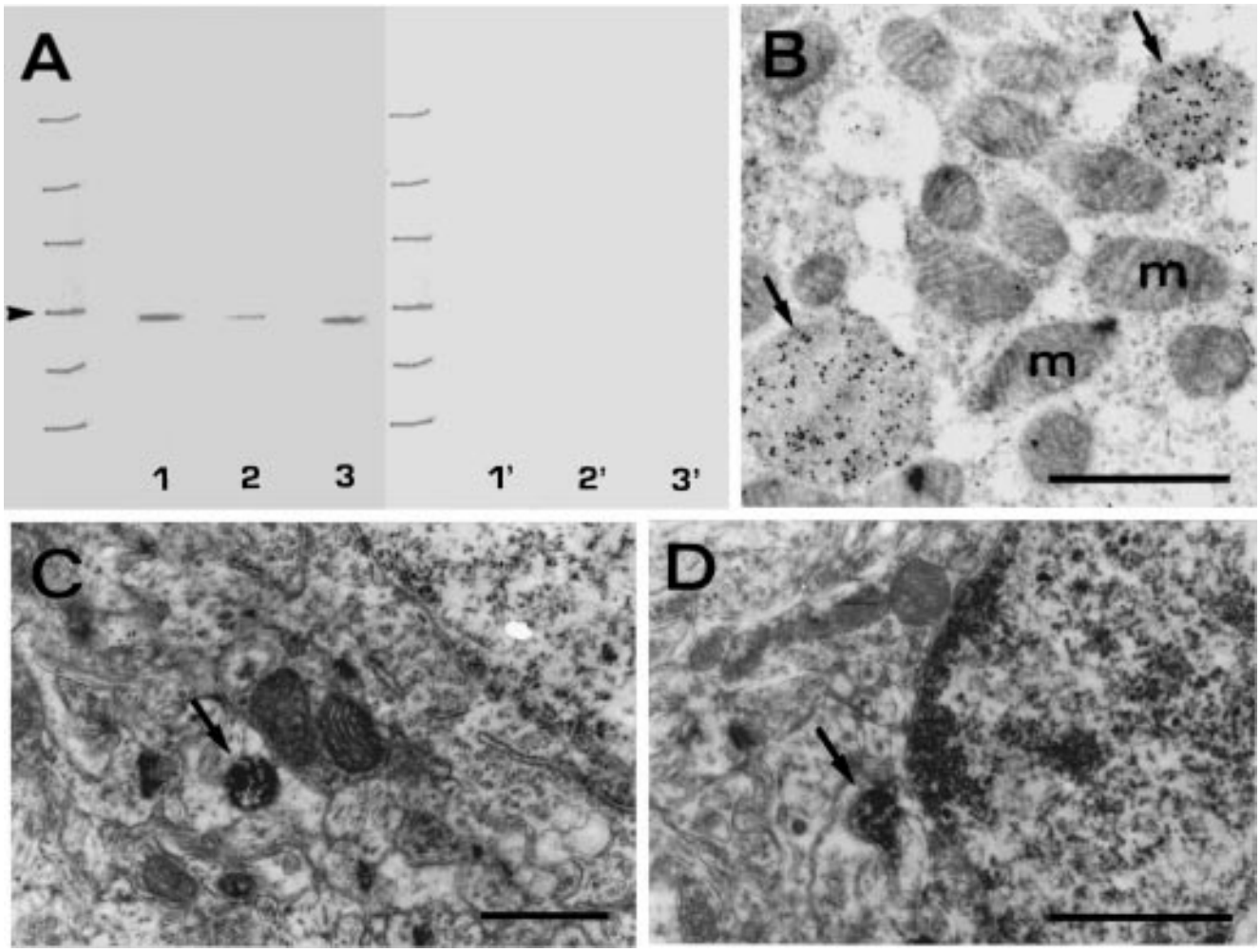

Fig. 1. (A) Immunoblotting with the affinity-purified anti-D-AAO polyclonal antibody. Lane 1, hog kidney D-AAO (20 ng protein). Lane 2, rat brain total homogenate (50 μg protein). Lane 3, rat liver total homogenate (25 μg protein). Only one immunoreactive band at 40 kDa is recognized by our antibody. Lanes 1′-3′, same as in lanes 1-3, but incubated with primary antibody preadsorbed with excess antigen. In these conditions no bands are visible. (B) Post-embedding immunoelectron microscopy of rat kidney with the anti-D-AAO antibody. Portion of a proximal convoluted tubule cell containing two immunogold labelled peroxisomes (arrows). Label is absent from other cellular compartments. m, mitochondria. (C), (D) Pre-embedding immunoelectron microscopy of rat brain with anti-D-AAO antibody, revealed with DAB. Portions of a neocortical neuron (C) and of a cerebellar astrocyte (D) showing immunostained peroxisomes (arrows). Other cellular compartments, as the nucleus, or mitochondria, are devoid of immunoprecipitate. Scale bars = 1 μm.

& Oertel, 1985) (Fig. 3A). In the remainder of the telencephalon, the septal nuclei and the basal ganglia, especially the ventral pallidum, are among the richest in D-AAO positive neurons (Fig. 3B–D). Concerning the caudate-putamen, only scattered medium- to large-sized cells probably corresponding to the cholinergic interneurons, show dense immunoreaction product, while the medium spiny neurons are only faintly stained (Fig. 3D). Other immunoreactive centers include the medial and anteromedial preoptic nuclei and the supraoptic nucleus (Fig. 4A). In the hippocampal formation, pyramidal neurons of fields CA1 and CA3, granule cells of the dentate gyrus, and many interneurons scattered in all the layers and in the subiculum are immunopositive (Fig. 4B–D).

In the diencephalon, neurons of the reticular thalamic nucleus are strongly immunoreactive, while other ventral and dorsal thalamic nuclei are weakly positive (Fig. 4E). Intensely stained neurons are also present in the zona incerta and subthalamic nucleus (Fig. 4F). The hypothalamus also displays differentiated levels of D-AAO immunoreactivity, with the strongest staining occurring in the paraventricular nucleus (Fig. 5A), periventricular nucleus, and bed nucleus of the anterior commissure. Additionally, a small group of medium-sized cells, peculiarly located in a parafornical position, shows intense immunoreactivity (Fig. 5B). These cells, which do not precisely correspond to any of the nuclei classically described in this area, appear instead very similar in location to those previously

Table 1. Distribution of D-AAO immunoreactivity in rat brain.

TELENCEPHALON		Anterodorsal nucleus	+++	Superior olivary complex:	
Main olfactory bulb:		Paraventricular nucleus	++	Nucleus of the trapezoid body	++
Glomerular layer	+	Paratenial nucleus	++	Medial superior olive	+
External plexiform layer	++	Paracentral nucleus	++	Lateral superior olive	+
Mitral cells	+++	Ventral nuclei	+	Rostral periolivary nucleus	++
Internal granular layer	+	Lateral nuclei group	+	Superior paraolivary nucleus	++
Anterior olfactory nucleus:		Rhomboid nucleus	++	Cranial motor nuclei:	
Layer 1a	++	Intralaminar and		Trochlear nucleus	++
Layer 3	+++	midline nuclear group	+	Trigeminal motor nucleus	++
Piriform cortex	+++	Habenula (medial nucleus)	++	Abducens nucleus	+++
Endopiriform nucleus		Zona incerta	++	Facial nucleus	++++
and claustrum	++	Subthalamic nucleus	+++	Ambiguus nucleus	++++
Olfactory tubercle	++	Hypothalamus:		Dorsal motor nucleus	
Tenia tecta	++	Paraventricular nucleus	+++	of the vagus	++++
Major island of Calleja	+	Periventricular nucleus	+++	Hypoglossal nucleus	+++
Entorhinal cortex	+	Bed nucleus of the		Spinal trigeminal nucleus	++++
Neocortex:		anterior commissure	++++	Cochlear nuclei:	
Layer II (pyramidal cells)	++	Unidentified parafornical cells	++++	Ventral cochlear nucleus	+++
Layer V (pyramidal cells)	+++	Mammillary nuclei	++	Dorsal cochlear nucleus	++
Layer VI (small interneurons)	+++			Vestibular nuclei:	
All layers (scattered interneurons)	+++	MESENCEPHALON		Lateral vestibular nucleus	++++
Stratum oriens, piramidalis,		Superior colliculus:		Spinal vestibular nucleus	++++
radiatum and lacunosum-		Superficial gray layer	++	Medial vestibular nucleus	++
moleculare (small interneurons)	++	Intermediate gray layer	++++	Superior vestibular nucleus	+
Subicular complex		Deep gray layer	++	Precerebellar nuclei:	
(small interneurons)	+++	Inferior colliculus:		Nucleus of Roller	++
Hippocampal CA3 region		Central nucleus	+++	Prepositus hypoglossal nucleus	++
(pyramidal cells)	+++	Cortex	+++	External cuneate nucleus	+++
Hippocampal CA1 region		Central gray	+++	Inferior olive	+++
(pyramidal cells)	+++	Tegmental nuclei:		Cerebellar cortex:	
Dentate gyrus (granule cells)	+	Anterior tegmental area	++	Purkinje cells	+/++++
Basal ganglia:		Subpeduncular tegmental nucleus	++	Golgi cells	+++
Caudate-putamen (scattered		Dorsal tegmental nucleus	++	Cerebellar nuclei:	
medium-to-large-sized neurons)	+++	Laterodorsal tegmental nucleus	++	Medial cerebellar nucleus	+++
Accumbens nucleus	+	Red nucleus, magnocellular part	++++	Interpositus cerebellar nucleus	+++
Globus pallidus	+	Locus ceruleus	++	Lateral cerebellar nucleus	+++
Entopeduncular nucleus	+++	Substantia nigra:Pars reticulata	+++	Dorsal column nuclei:	
Ventral pallidum	+++	Substantia nigra:Pars lateralis	++	Cuneate nucleus	+
Substantia innominata	+	Substantia nigra:Pars compacta	++	Nucleus gracilis	++
Basal nucleus of Meynert	+++	Ventral tegmental area	+	Area postrema	+
Septum:		Oculomotor nucleus	+++		
Medial septal nucleus	+++	Interpeduncular nucleus	++	GLIAL CELLS	
Nucleus of the vertical limb		Raphe nuclei	+++	Lateral olfactory tract	+
of the diagonal band	+++	Mesencephalic reticular nuclei	+++	Corpus callosum	++
Nucleus of the horizontal limb		Nucleus of the mesencephalic		Internal capsule	+
of the diagonal band	+++	tract of the trigeminal nerve	++++	External capsule	++
Lateral septal nucleus	+	Lateral parabrachial nucleus	+	Cerebral peduncle	+
Septohippocampal nucleus	+			Fornix	+
Septofimbrial nucleus	+	RHOMBENCEPHALON		Fimbria	+
Triangular septal nucleus	++	Pontine nuclei	+++	Stria medullaris thalami	+
Anteromedial preoptic nucleus	+++	Reticulotegmental nucleus	++	Optic chiasm	+++
Medial preoptic nucleus	++	Reticular formation:		Lateral lemniscus	+++
Medial preoptic area	+	Gigantocellular reticular nucleus	++++	Pyramidal tract	++
Supraoptic nucleus	+++	Pontine reticular nuclei	+++	Spinal trigeminal tract	+++
		Lateral reticular nucleus	+++	Inferior cerebellar peduncle	++
		Rostroventrolateral reticular		Bergmann glia	+++
DIENCEPHALON		nucleus	++++	Ependyma	−/+++
Thalamus:		Nucleus of Darkschewitsch	++	Tanycytes of III ventricle	+++
Reticular thalamic nucleus	+++	Nuclei of the lateral lemniscus	++		

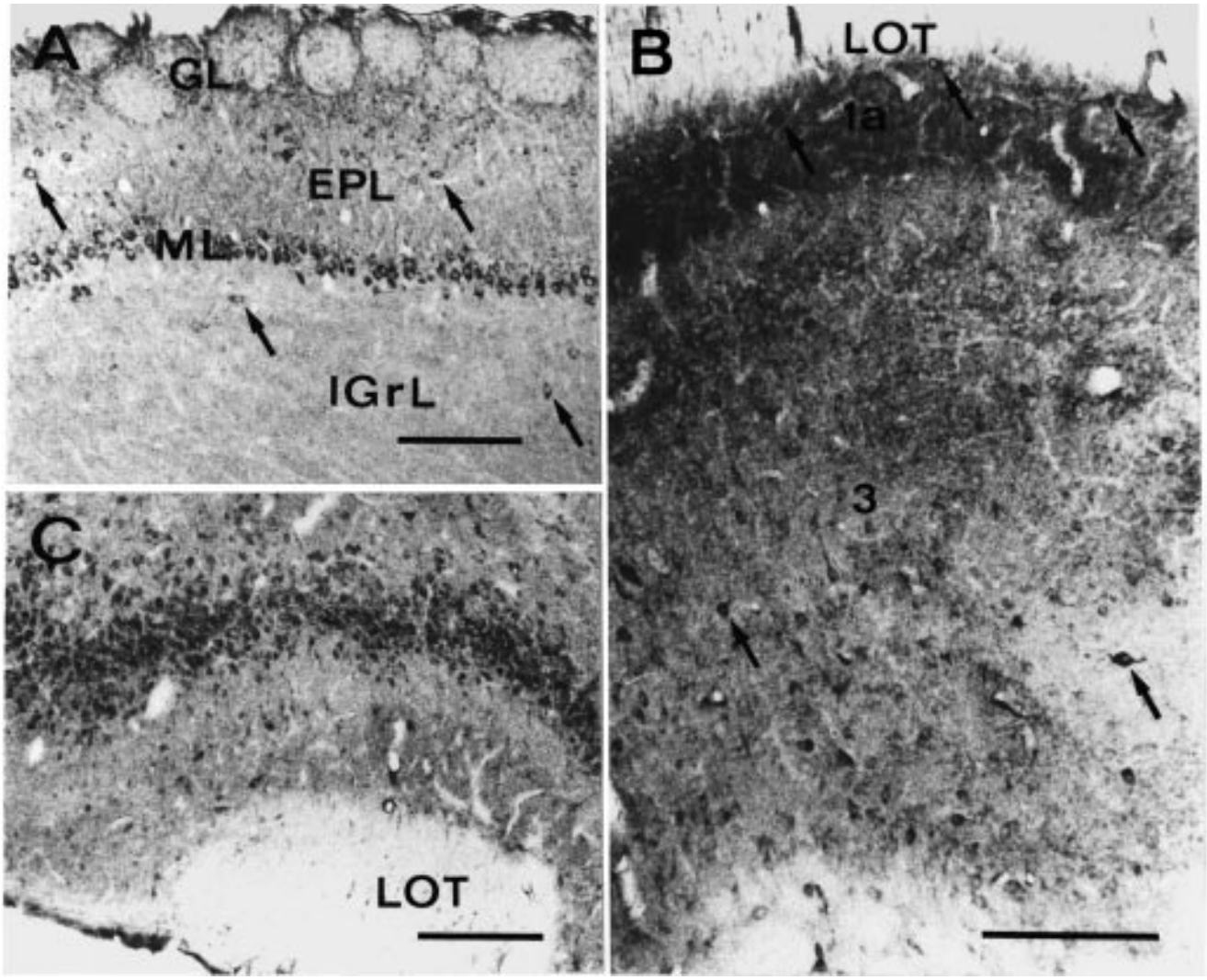

Fig. 2. Coronal sections of rat telencephalon. D-AAO immunocytochemistry. (A) Main olfactory bulb. Positive neurons include mitral cells (ML) and cells (arrows) in the external plexiform (EPL) and internal granular (IGrL) layers. GL, glomerular layer. (B) Anterior olfactory nucleus. Arrows indicate immunoreactive cells of layers 1a and 3. LOT, lateral olfactory tract. (C) Piriform cortex. LOT, lateral olfactory tract. Scale bars = 200 μm.

identified by catalase immunocytochemistry (Moreno *et al.*, 1995).

In the mesencephalon, neurons located in both the superficial and intermediate divisions of the superior colliculus show dense immunoreaction product (Fig. 5C). The central nucleus and the external cortex of the inferior colliculus, as well as the central gray, are also positive (Fig. 5D and E). The red nucleus represents one of the most intensely stained centers of the whole brain (Fig. 6A). In the substantia nigra, the pars compacta and particularly the pars reticulata, are D-AAO positive neurons (Fig. 6B). Other mesencephalic immunolabelled areas include the raphe nuclei (Fig. 6C).

High immunoreactivity levels occur in numerous regions in the rhombencephalon. The cerebellum shows strong positivity in several neuronal subtypes, including Golgi neurons of the granular layer (Fig. 7A and B). Purkinje cells are also immunoreactive, although their positivity is not uniform throughout the cortex (Fig. 7A). They show higher staining intensities

Fig. 3. Coronal sections of rat telencephalon. D-AAO immunocytochemistry. (A) Cerebral cortex. Numerous intensely immunostained neurons are visible throughout the layers. Note the immunonegative nuclei, particularly evident in the giant pyramidal cells of the fifth layer (V). (B) Septal complex. MS, medial septal nucleus; VDB and HDB, vertical and horizontal nucleus of the diagonal band of Broca. (C) VP, Ventral pallidum; Tu, olfactory tubercle. (D) Caudate putamen. The immunoreaction product is found in medium-to-large sized neurons (arrows). Scale bars = 200 μm.

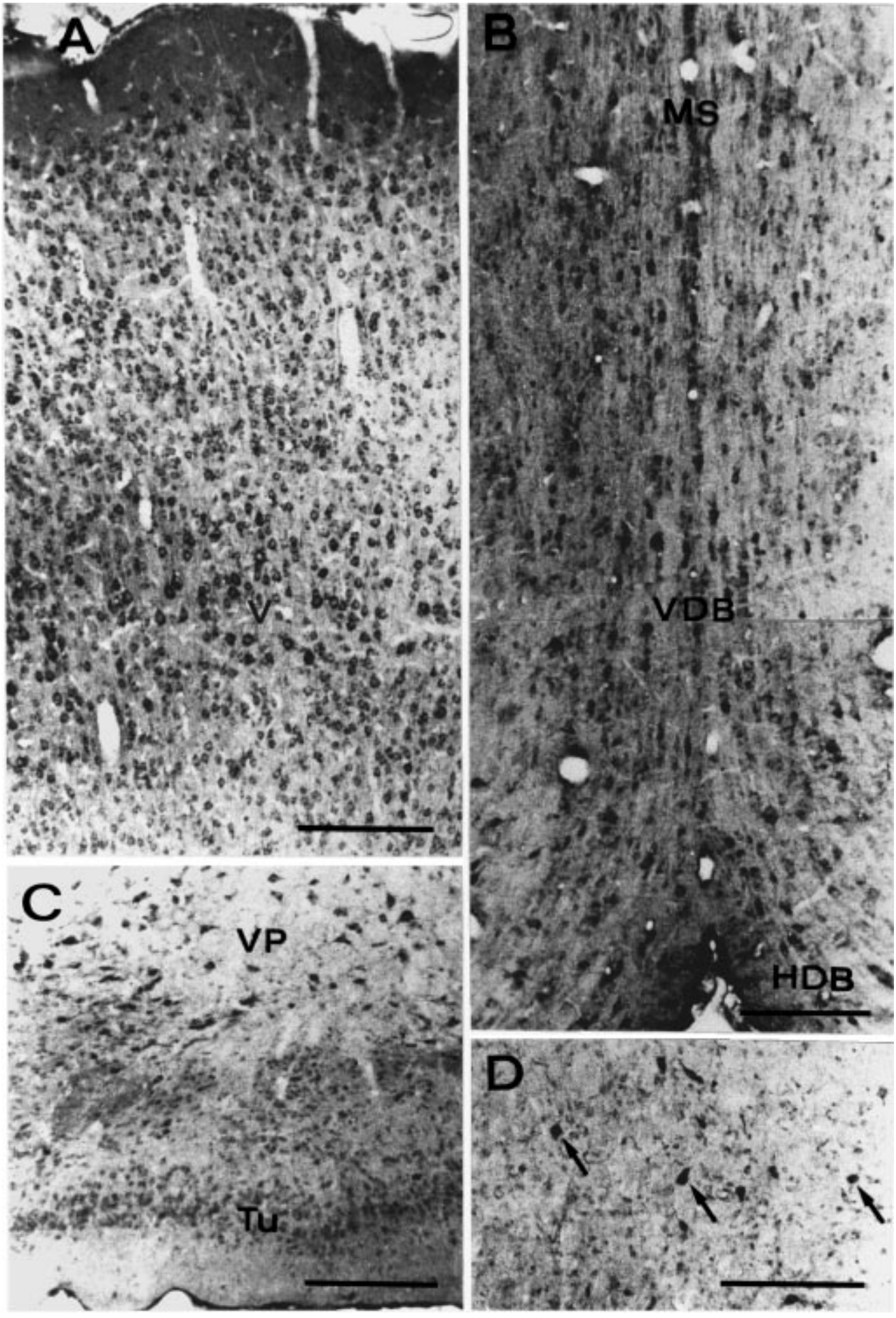
A
V
B
MS
VDB
HDB
C
VP
Tu
D

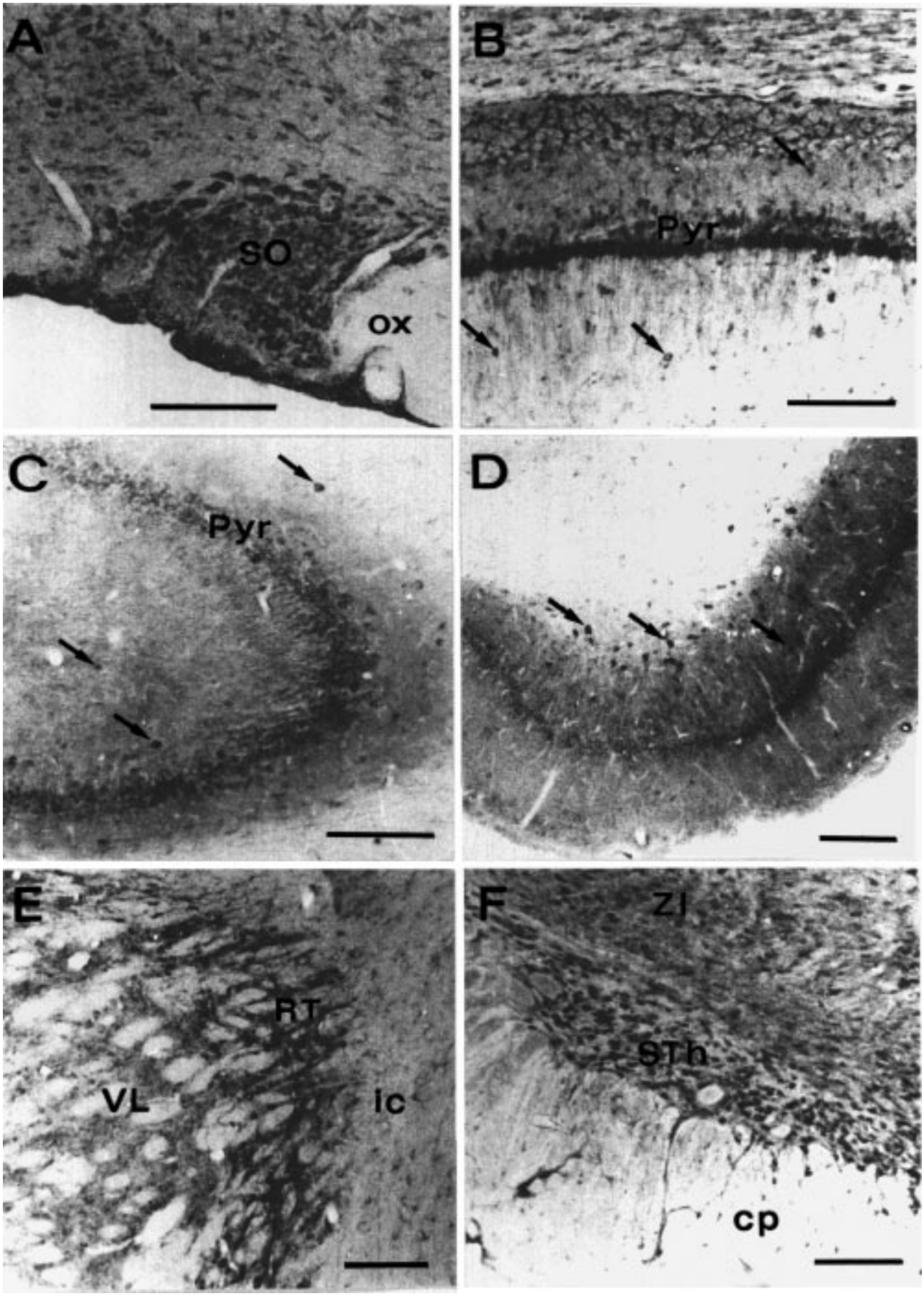
A
SO
ox
B
Pyr
C
Pyr
D
E
RT
VL
lc
F
ZI
STh
cp

in some folia, or parts of them, and much weaker—if not absent—staining in others (Fig. 7A). Granule, basket, and stellate neurons have almost negligible immunoreactivity. Moderate to high concentrations of immunoreaction product are found in neurons belonging to the deep cerebellar nuclei and vestibular nuclei, with the lateral vestibular nucleus displaying the most intense staining (Fig. 7C and D). Neurons of the reticular formation are strongly immunopositive, especially the gigantocellular nucleus (Fig. 8A and C). Cranial motor nuclei, especially the ambiguous, facial, and dorsal motor nuclei, show very strong staining (Fig. 8A–D). Other positive centers include pontine nuclei, cochlear nuclei, inferior olive, sensory trigeminal nuclei, and nuclei of the trapezoid body (Fig. 8E and F).

GLIA

Among glia, the astrocyte is the most intensely immunoreactive cell type. Positive astrocytes are found throughout the brain, including gray and white matter. In the forebrain, the corpus callosum, the optic chiasm, and the external capsule show strong immunolabelling of astrocytes (Fig. 9A, B). The largest numbers of positive cells and the strongest immunostaining are observed in the hindbrain, especially in the cerebellum (Figs. 7B, 8E and F and 9C).

The Golgi-Bergmann glia of the cerebellar cortex exhibit intense positivity which extends from the cell body to the radial processes (Fig. 7B). Other radial glia, e.g. tanycytes bordering the third ventricle and the median eminence, show strong and specific staining (Fig. 9D).

Immunoreactivity is also observed in ependymal cells (Figs. 5A and 8D), but no immunopositive oligodendrocytes are evident.

Discussion

In the present paper we report the first complete map of D-AAO in rat brain, obtained by means of an intensification immunocytochemical procedure (Adams, 1992), which proved highly sensitive in detecting peroxisomal enzymes (Moreno *et al.*, 1995, 1997). We show that D-AAO is localized in both neurons and glia, albeit at different concentrations depending on the cell type and regional location. The diffuse appearance of the cytoplasmic staining could be either due to the small size of peroxisomes in neural cells, which are hardly recognized at the LM level in relatively thick sections, or, most probably, to the fact that D-AAO protein easily leaks out from peroxisomes, as also biochemically described (Gaunt & De Duve, 1976; Cimini *et al.*, 1998).

DISTRIBUTION OF D-AAO IMMUNOREACTIVITY IN GLIAL CELLS

Astrocytes and radial glia are the glial cell types richest in D-AAO. Ependymal cells also contain moderate amounts of the enzyme, while other glia are apparently immunonegative. Regional differences have also been detected. Astroglial cells of the caudal brainstem and the cerebellum are generally more immunoreactive than those in the forebrain. These results are compatible with previous studies utilizing histochemical techniques (Gaunt & De Duve, 1976; Arnold *et al.*, 1979; Horiike *et al.*, 1994; Schell *et al.*, 1995). Regarding radial glia, Golgi-Bergmann cells of the cerebellar cortex and tanycytes bordering the third ventricle and median eminence show distinct immunoreactivity. This result is in agreement with previous histochemical findings on rat Bergmann glia (Weimar & Neims, 1977; Arnold *et al.*, 1979; Horiike *et al.*, 1987) and on frog retinal Muller cells (Beard *et al.*, 1988).

DISTRIBUTION OF D-AAO IMMUNOREACTIVITY IN NEURONS

Many neurons were observed to contain D-AAO. This finding is novel, as the enzyme was previously reported to be absent from neurons, based on histochemical studies (Arnold *et al.*, 1979; Horiike *et al.*, 1994; Schell *et al.*, 1995). A possible explanation of this difference is that histochemical techniques are based on enzymatic activity, while immunohistochemistry allows detection of the protein even if it is not active. Although the histochemical method may be extremely sensitive, fixation and subsequent procedures may impair some of the D-AAO activity. Furthermore, the natural substrate for D-AAO has not yet been identified; therefore, D-proline used for histochemical localization (Arnold *et al.*, 1979; Horiike *et al.*, 1985; Beard *et al.*, 1988) may not be the most suitable substrate to reveal D-AAO activity in cells other than astrocytes. Actually, other substrates, such as thiazolidine-2-carboxylic acid, proved effective in revealing D-AAO activity both biochemically (Fitzpatrick & Massey, 1982; Hamilton, 1985) and cytochemically (Angermuller, 1989; Jules *et al.*, 1991).

Fig. 4. Coronal sections of rat telencephalon (A–D) and diencephalon (E, F). D-AAO immunocytochemistry. (A) SO, supraoptic nucleus; ox, optic chiasm. (B) CA1 region of the hippocampus. Pyramidal cells (Pyr) are highly immunoreactive. Arrows indicate positive neurons distributed in all the layers. (C) CA3 region of the hippocampus, showing positive pyramidal cells (Pyr) and scattered neurons (arrows). (D) Subiculum. Arrows indicate immunostained neurons. (E) Thalamus. RT, reticular thalamic nucleus; VL, ventrolateral thalamic nucleus. Note also immunorective glial cells of the internal capsule (ic). (F) STh, subthalamic nucleus; ZI, zona incerta; cp, cerebral peduncle. Scale bars = 200 μm.

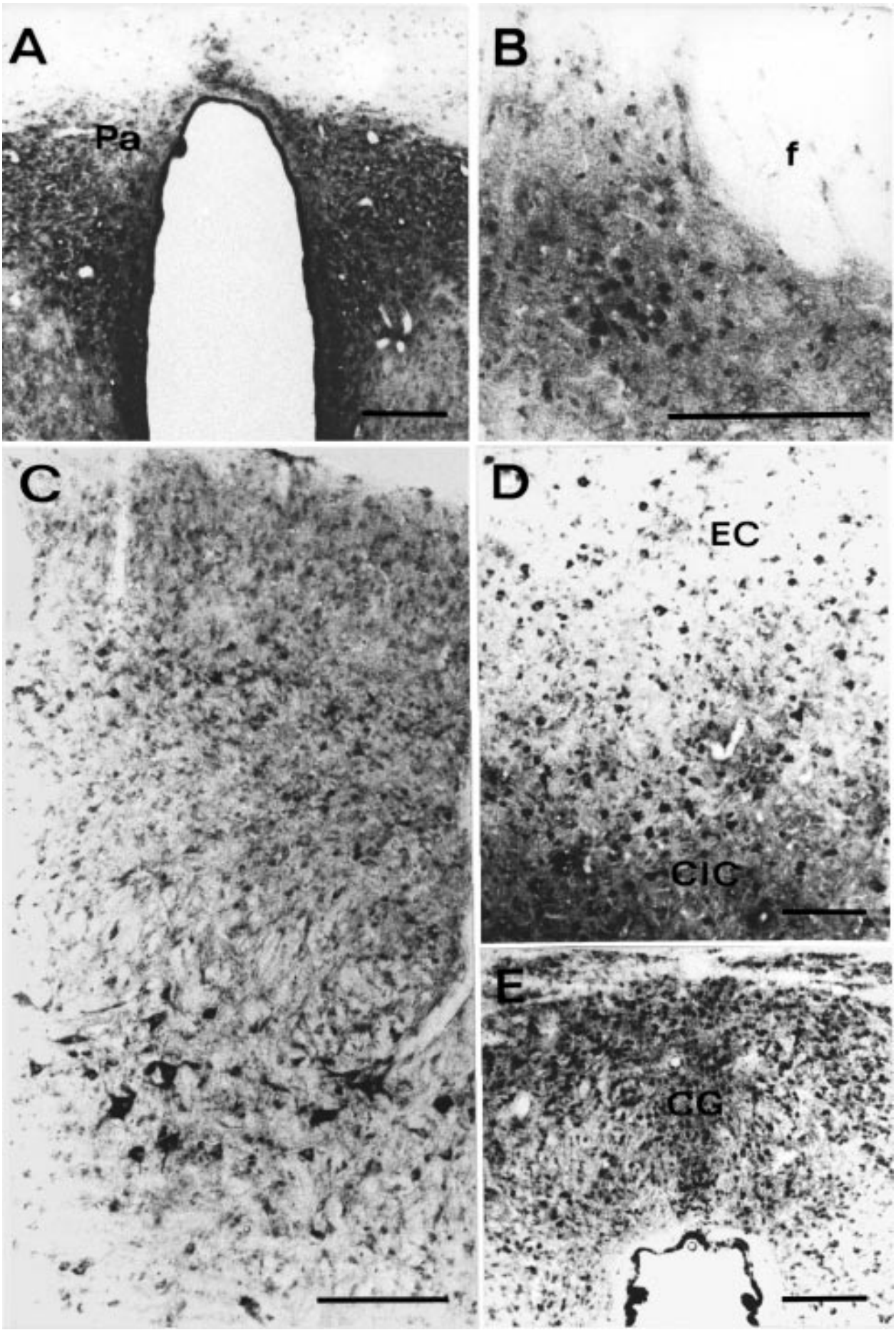
A
Pa
B
f
C
D
EC
CIC
E
CG

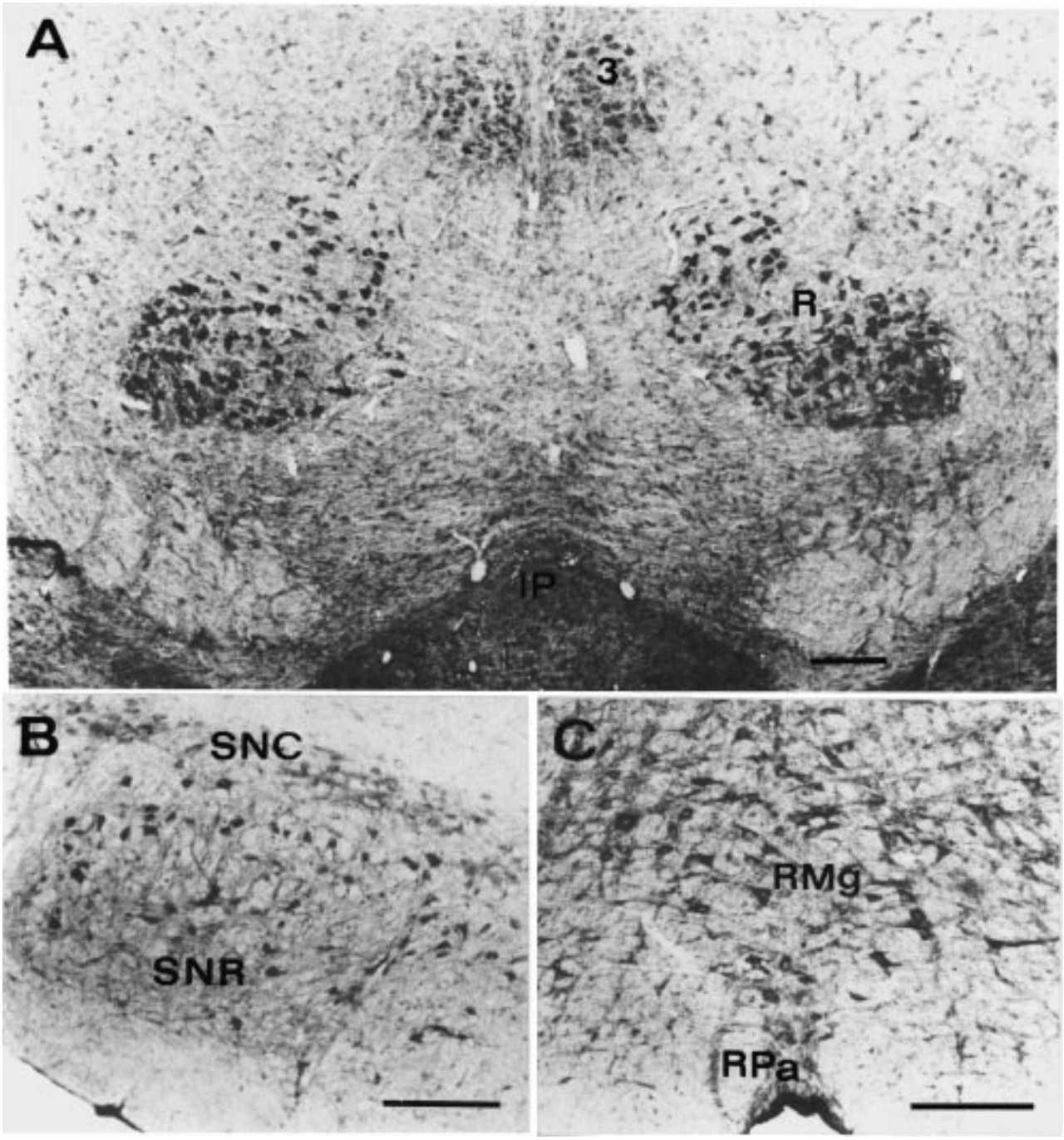

Fig. 6. Coronal sections of rat mesencephalon. D-AAO immunocytochemistry. (A) The magnocellular part of the red nucleus (R) is extraordinarily positive. 3, oculomotor nucleus; IP, interpeduncular nucleus. (B) Substantia nigra. SNR, pars reticulata; SNC, pars compacta. (C) Raphe nuclei. RMg, magnus nucleus; RPa, pallidus nucleus. Scale bars = 200 μm.

Fig. 5. Coronal sections of rat diencephalon (A, B) and mesencephalon (C–E). D-AAO immunocytochemistry. (A) Hypothalamus. Pa, paraventricular hypothalamic nucleus. Note the intense staining in ependymal cells bordering the third ventricle. (B) Hypothalamus. Small group of immunopositive neurons close to the fornix (f). (C) Superior colliculus. Note immunonegative nuclei. (D) Inferior colliculus. EC, external cortex; CIC, central nucleus. (E) Central gray (CG) neurons are intensely immunopositive. Scale bars = 200 μm.

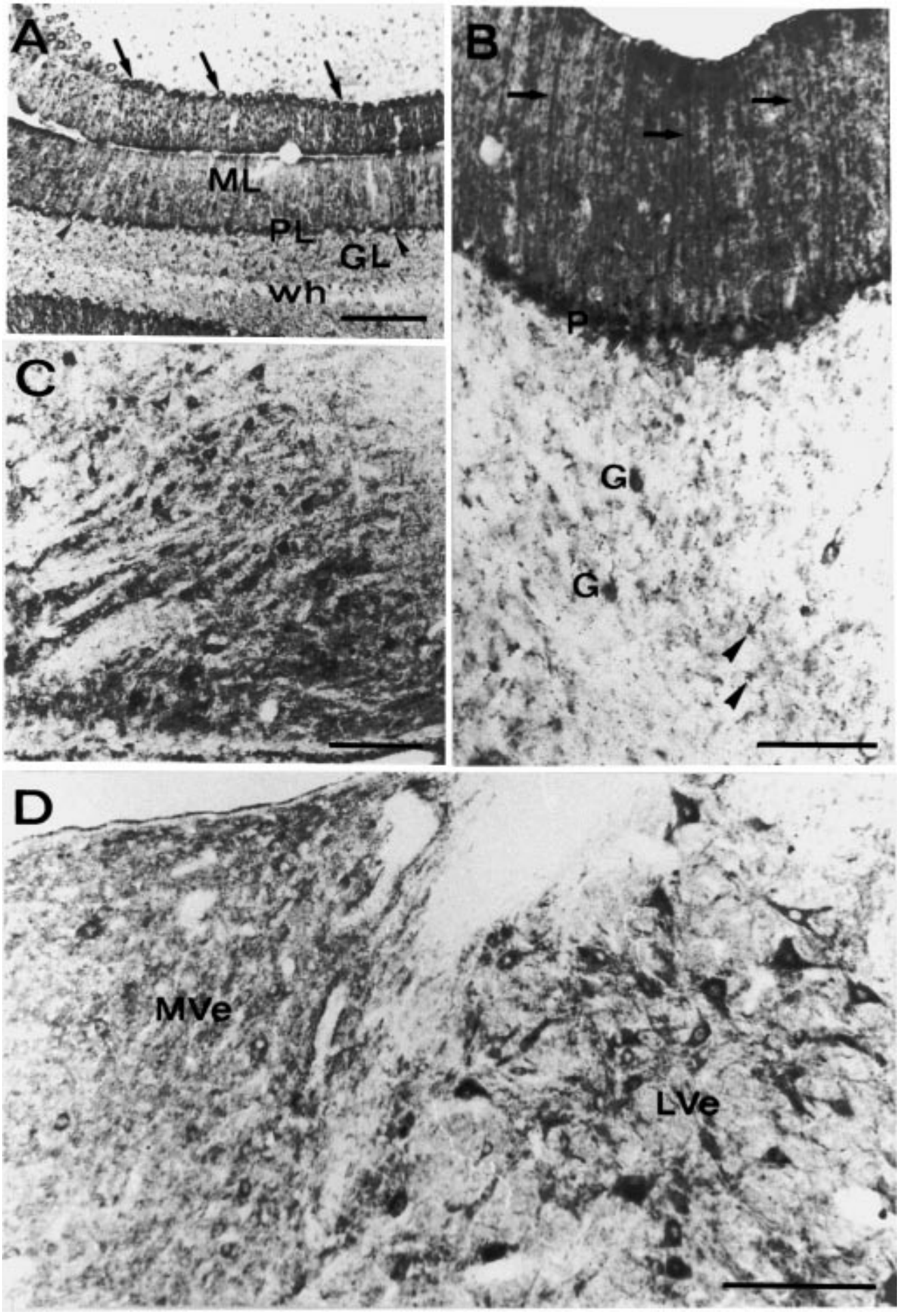
A
ML
PL
GL
wh
B
P
G
G
C
D
MVe
LVe

D-AAO neuronal immunoreactivity is generally stronger in the hindbrain than in the forebrain. However, numerous forebrain neuronal subtypes (e.g., mitral cells of the olfactory bulb, cortical and hippocampal neurons, and neurons of the septum) display high staining intensities. Thus, generalizations on the regional D-AAO distribution based solely on brain gross anatomy are inadequate, at least as far as neurons are concerned.

To get some insight into the physiological significance of the differential expression in specific neuronal populations, we considered possible relationships between the abundance of the enzyme and some characteristic of the D-AAO positive neurons. However, neither the specific mediator, nor the cell size or the projection site are likely to underlie these differences. In fact, reaction product is found in neurons known to be GABAergic (e.g., Golgi and Purkinje neurons), cholinergic (e.g., motor neurons), catecholaminergic (e.g., substantia nigra pars compacta), and glutamatergic (e.g., red nucleus); in large neurons (e.g., mitral cells) and small neurons (e.g., layer VI neocortical cells); in interneurons and principal neurons of numerous regions (e.g., neocortex and hippocampus). Studies dealing with the identification of the physiological role(s) of D-AAO may help in the interpretation of our results.

CONCLUDING REMARKS

Recent results indicate a function for the enzyme in regulating the levels of D-serine, which acts as an endogenous modulator of the NMDA-receptor complex. Our results on the localization of D-AAO, compared with those of Schell *et al.* (1995) on the distribution of D-serine and of the NMDA-receptors, agree with this hypothesis. However, the possibility that D-AAO in nervous tissue may serve some other, still unknown function, cannot be excluded. In this context, it should be recalled that the carbon skeletons generated by the oxidative deamination of serine and a number of other amino acids can be used for the synthesis of glucose through the process of gluconeogenesis (Mannaerts & van Veldoven, 1993). The proposal that D-AAO may use as substrate thiazolidine-2-carboxylate, the cysteamine-glyoxylate adduct, would imply that the enzyme may control the levels of these molecules (Hamilton, 1985). It is worth noting that peroxisomes, where D-AAO is localized, are also the major site for the metabolism of glyoxylate (Masters, 1997). Finally, since D-AAO is a peroxisomal enzyme, it is relevant to compare its localization with that of other peroxisomal proteins, such as catalase, which is widely considered a marker for peroxisomes. The comparison between D-AAO distribution, as described in this paper, and the immunocytochemical map that we previously obtained for catalase (Moreno *et al.*, 1995) indicates that immunoreactivity is similar for the two enzymes. In fact, many brain centers (namely ventral pallidum, septal nuclei, reticular thalamic nucleus, red nucleus, cranial motor nuclei, deep cerebellar nuclei, vestibular nuclei, and most of the other brainstem nuclei) show exactly matching patterns of immunostaining. On the other hand, some D-AAO immunoreactive neurons, such as mitral cells, were described as catalase-negative; in contrast, in other brain regions, such as the globus pallidum, we found cells low in D-AAO to be strongly catalase positive (Moreno *et al.*, 1995).

Comparing the distributions of D-AAO and catalase immunoreactivities may also be extended to glial cells. Catalase is present in virtually all glia, while D-AAO is present mostly in astrocytes. Thus, a more restricted expression of D-AAO is supported by this and other studies (Horiike *et al.*, 1994).

The existence of D-AAO-negative, catalase-positive cells on one hand, and of D-AAO-positive, catalase-negative cells on the other, suggested by this investigation, raises important questions concerning peroxisomes and, specifically, their enzymatic content. Previous studies (Gaunt & de Duve 1976; Arnold *et al.*, 1979; Cimini *et al.*, 1993, 1998) demonstrated the existence in nervous tissue of both catalase-rich D-AAO-poor and catalase-poor D-AAO-rich peroxisomes.

All these findings, together with the increasing evidence that catalase may no longer be considered a universal marker for peroxisomes (van Roermund *et al.*, 1995), point to the conclusion of peroxisomal heterogeneity in nervous tissue.

Acknowledgments

The authors thank Dr. Enrico Mugnaini for critical reading of the manuscript and helpful discussion, Dr. Stefania Stefanini for immunogold analysis, Prof. Annarosa Ciofi Luzzatto for the EM facilities at the Interdepartmental Laboratory of Electron Microscopy (LIME,

Fig. 7. Coronal sections of rat rhombencephalon. D-AAO immunocytochemistry. (A) Cerebellar cortex showing two contiguous folia. ML, molecular layer; PL, Purkinje cell layer; GL, granular layer; wh, white matter. Purkinje cells of the upper folium show dense cytoplasmic immunoreaction product (arrows), while those of the lower folium are practically negative (arrowheads). Scale bar = 200 μm. (B) Higher magnification of the cerebellar cortex. Purkinje cells (P) show discontinuous immunoreactivity. G, Golgi neurons in the granular layer. Note positive Bergmann glial processes in the molecular layer (arrows) and astrocytes in the granular layer (arrowheads). Scale bar = 100 μm. (C) Medial cerebellar nucleus. Scale bar = 200 μm. (D) Vestibular nuclei. MVe, medial vestibular nucleus; LVe, lateral vestibular nucleus. Note immunonegative nuclei. Scale bar = 200 μm.

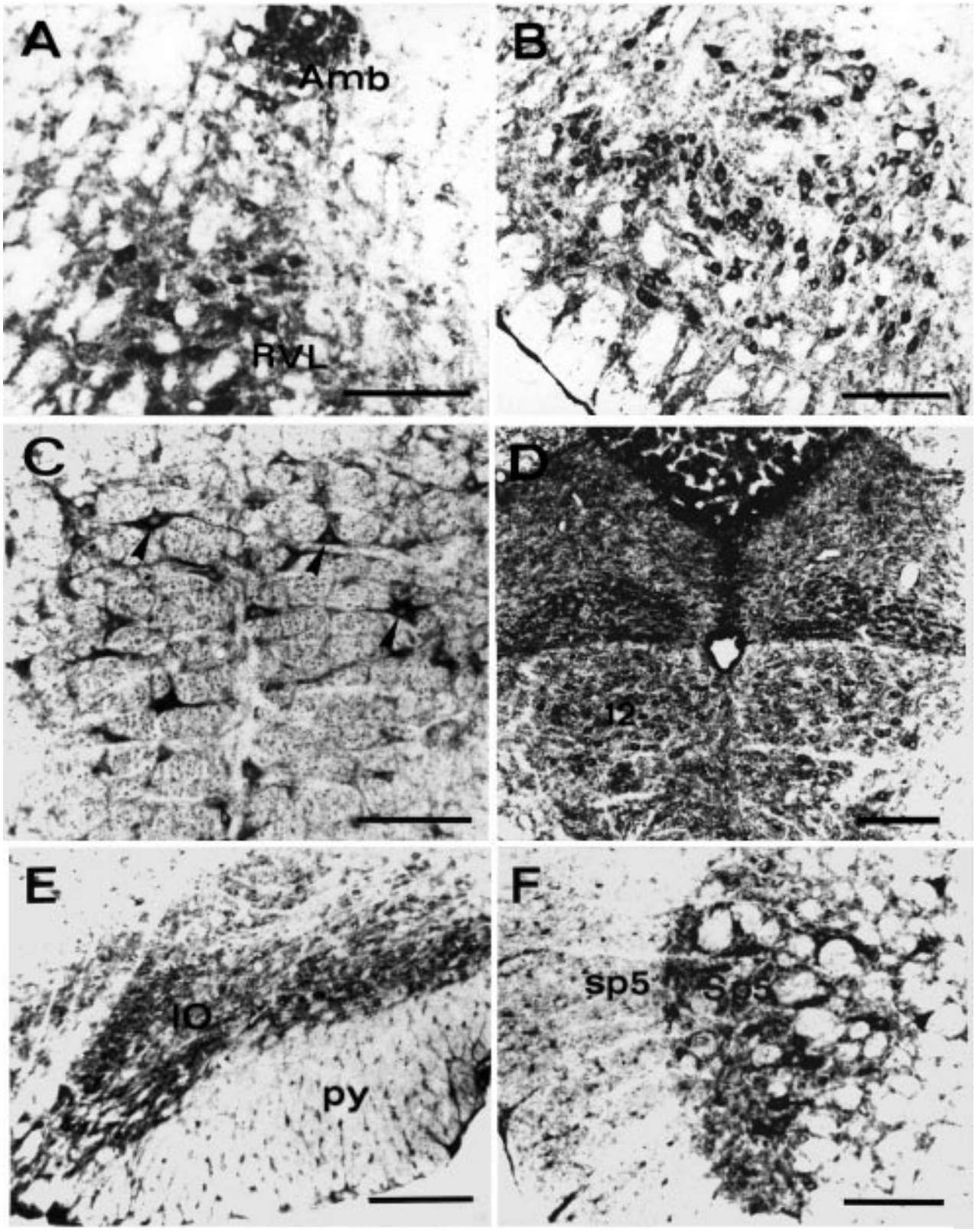

Fig. 8. Coronal sections of rat rhombencephalon. D-AAO immunocytochemistry. (A) Amb, ambiguous nucleus; RVL, rostroventrolateral reticular nucleus. (B) Facial nucleus. (C) Arrowheads indicate neurons of the gigantocellular reticular nucleus, which show evident positivity in their somata and processes, but not in their nuclei. Note the numerous positive axons. (D) 10, dorsal motor nucleus of the vagus nerve; 12, hypoglossal nucleus. (E) Inferior olive (IO). Note also immunoreactive glial cells of the pyramidal tract (py). (F) Neuronal and glial elements of the spinal trigeminal tract (sp5) and nucleus (Sp5) show strong immunostaining. Scale bars = 200 μm.

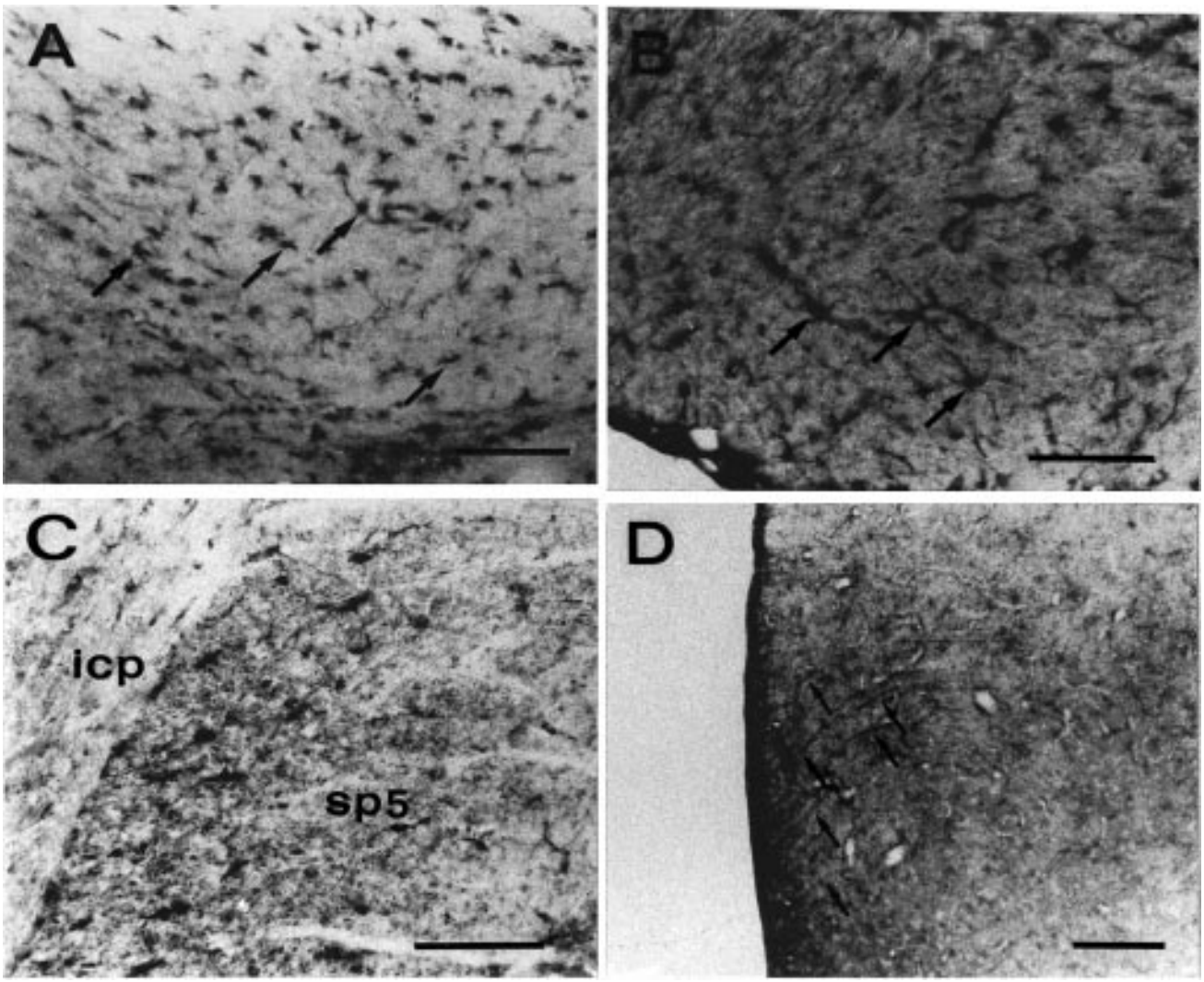

Fig. 9. Coronal sections of rat brain. D-AAO immunocytochemistry. (A) Corpus callosum. Many immunoreactive astroglial cells are visible (arrows). (B) Optic chiasm. Note that the immunoreaction product extends from the cell body to the processes of astrocytes (arrows). (C) icp, inferior cerebellar peduncle; sp5, spinal trigeminal tract. (D) Tanycytes of the third ventricle, showing positive staining in their long processes (arrows). Scale bars = 100 μm.

University ROMA TRE-Rome, Italy), and Dr. Pierpaolo Aimola for technical assistance. This research was supported by CNR grant No. 97.04447.CT04, and partially by the European Concerted Action Peroxisomal leukodystrophy BMH4-CT96.1621.

References

ADAMS, J. C. (1992) Biotin amplification of biotin and horseradish peroxidase signals in histochemical stains. *Journal of Histochemistry and Cytochemistry* **40**, 1457–1463.

ANGERMULLER, S. (1989) Peroxisomal oxidases: cytochemical localization and biological relevance. *Progress in Histochemistry and Cytochemistry* **20**, 1–63.

ARNOLD, G., LISCUM, L. & HOLTZMAN, E. (1979) Ultrastructural localization of D-amino acid oxidase in microperoxisomes in the rat nervous system. *Journal of Histochemistry and Cytochemistry* **27**, 735– 745.

BEARD, M. E., DAVIES, T., HOLLOWAY, M. & HOLTZMAN, E. (1988) Peroxisomes in pigment epithelium and Muller cells of amphibian retina possess D-amino acid oxidase as well as catalase. *Experimental Eye Research* **47**, 795–806.

BRIGHT, H. J. & PORTER, D. J. T. (1975) Flavoprotein oxidases. In *The Enzymes*, Vol. 12: (edited by BOYER, P. D.), pp. 421–505. New York: Academic Press.

CIMINI, A. M., MORENO, S., SERAFINI, B. & CERÙ, M. P. (1993) Purification of peroxisomal fraction from rat brain. *Neurochemistry International* **23**, 249–260.

CIMINI, A. M., SINGH, I., FARIOLI VECCHIOLI, S., CRISTIANO, L. & CERÙ, M. P. (1998) Presence of heterogeneous peroxisomal populations in the rat nervous tissue. *Biochimica et Biophysica Acta* **1425**, 13–26.

D'ANIELLO, A., D'ONOFRIO, G., PESCHETOLA, M., D'ANIELLO, G., VETERE, A., PETRUCELLI, L. & FISCHER, G. H. (1993) Biological role of D-amino acid oxidase and D-aspartate oxidase: effects of D-amino acids. *Journal of Biological Chemistry* **268**, 26941–26949.

D'ANIELLO, A., VETERE, A. & PETRUCELLI, L. (1993a) Further study on the specificity of D-amino acid oxidase and of D-aspartate oxidase and time course for complete oxidation of D-amino acids. *Comparative Biochemistry and Physiology* **105 B**, 731–734.

DIXON, M. & KLEPPE, K. (1965) D-amino acid oxidase: II. Specificity, competitive inhibition and reaction sequence. *Biochimica et Biophysica Acta* **96**, 368–382.

FEDELE, E., BISAGLIA, M. & RAITERI, M. (1997) D-serine modulates the NMDA receptor/nitric oxide/cGMP pathway in the rat cerebellum during in vivo microdialysis. *Naunyn-Schmiedeberg's Archives Pharmacology* **355**, 43–47.

FITZPATRICK, P. F. & MASSEY, V. (1982) Thiazolidine-2-carboxylic acid, an adduct of cysteamine and glyoxilate, as a substrate for D-amino acid oxidase. *Journal of Biological Chemistry* **257**, 1166–1171.

GAUNT, G. L. & DE DUVE, C. (1976) Subcellular distribution of D-amino acid oxidase and catalase in rat brain. *Journal of Neurochemistry* **26**, 749–759.

HAMILTON, G. A. (1985) Peroxisomal oxidases and suggestions for the mechanism of action of insulin and other hormones. *Advances in Enzymology* **57**, 85–178.

HASHIMOTO, A., NISHIKAWA, T., HAYASHI, T., FUJI, N., HARADA, K., OKA, T. & TAKAHASHI, K. (1992) The presence of free D-serine in rat brain. *FEBS Letters* **296**, 33–36.

HASHIMOTO, A., NISHIKAWA, T., OKA, T. & TAKAHASHI, K. (1993) Endogenous D-serine in rat brain: N-methyl-D-aspartate receptor-related distribution and aging. *Journal of Neurochemistry* **60**, 783–786.

HASHIMOTO, A., OKA, T. & NISHIKAWA, T. (1995) Anatomical distribution and post-natal changes in endogenous free D-aspartate and D-serine in rat brain and periphery. *European Journal of Neuroscience* **7**, 1657–1663.

HOLTZMAN, E. (1982) Peroxisomes in nervous tissue. *Annals of the New York Academy of Sciences* **386**, 523–525.

HORIIKE, K., ARAI, R., TOJO, H., YAMANO, T., NOZAKI, M. & MAEDA, T. (1985) Histochemical staining of cells containing flavoenzyme D-amino acid oxidase based on its enzymatic activity: application of a coupled peroxidation method. *Acta Histochemica et Cytochemica* **18**, 539–550.

HORIIKE, K., TOJO, H., ARAI, R., YAMANO, T., NOZAKI, M. & MAEDA, T. (1987) Localization of D-amino acid oxidase in Bergmann glial cells and astrocytes of rat cerebellum. *Brain Research Bullettin* **19**, 587–596.

HORIIKE, K., TOJO, H., ARAI, R., NOZAKI, M. & MAEDA, T. (1994) D-Aminoacid oxidase is confined to the lower brain stem and cerebellum in rat brain: regional differentiation of astrocytes. *Brain Research* **652**, 297–303.

JULES, R. S., KENNARD, J., SETLIK, W. & HOLTZMAN, E. (1991) Peroxisomal oxidation of thiazolidine carboxylates in firefly fat body, frog retina, and rat liver and kidney. *European Journal of Cell Biology* **55**, 94–103.

KONNO, R., SASAKI, M., ASAKURA, S., FUKUI, K., ENAMI, J. & NIWA, A. (1997) D-Amino-acid oxidase is not present in the mouse liver. *Biochimica et Biophysica Acta* **1335**, 173–181.

KONNO, R., UCHYAMA, S. & YASUMURA, Y. (1982) Intraspecies and interspecies variations in the substrate specificity of D-amino acid oxidase. *Comparative Biochemistry and Physiology* **71B**, 735–738.

KONNO, R. & YASUMURA, Y. (1983) Mouse mutant deficient in D-aminoacid oxidase activity. *Genetica* **103**, 277–284.

KONNO, R. & YASUMURA, Y. (1992) D-amino-acid oxidase and its physiological function. *International Journal of Biochemistry* **24**, 519–524.

KREBS, H. A. (1935) Metabolism of amino-acids. III. Deamination of amino-acids. *Biochemical Journal* **29**, 1620–1644.

LAEMMLI, E. K. (1970) Cleavage of structural proteins during the assembly of the head of the bacteriophage T4. *Nature* **227**, 680–685.

MANNAERTS, G. P. & VAN VELDHOVEN, P. P. (1993) Metabolic role of mammalian peroxisome. In *Peroxisomes. Biology and Importance in Toxicology and Medicine* (edited by GIBSON, G. & LAKE, B.), pp. 19–62. London: Taylor & Francis.

MASTERS, C. (1997) Gluconeogenesis and the peroxisome. *Molecular and Cellular Biochemistry* **166**, 159–168.

MORENO, S., MUGNAINI, E. & CERÙ, M. P. (1995) Immunocytochemical localization of catalase in the central nervous system of the rat. *Journal of Histochemistry and Cytochemistry* **43**, 1253–1267.

MORENO, S., NARDACCI, R. & CERÙ, M. P. (1997) Regional and ultrastructural immunolocalization of copper-zinc superoxide dismutase in rat central nervous system. *Journal of Histochemistry and Cytochemistry* **45**, 1611–1622.

MOSER, H. W. (1987) New approaches in peroxisomal disorders. *Developmental Neuroscience* **9**, 1–18.

MUGNAINI, E. & DAHL, A. L. (1983) Zinc-aldehyde fixation for light microscopic immunocytochemistry of nervous tissues. *Journal of Histochemistry and Cytochemistry* **31**, 1435.

MUGNAINI, E. & OERTEL, W. H. (1985) An atlas of the distribution GABAergic neurons and terminals in the rat CNS as revealed by GAD immunohistochemistry. In *Handbook of Chemical Neuroanatomy* (edited by BJORKLUND, A. & HOKFELT, T.) Vol. 4. Part I: pp. 436–608. New York: Elsevier.

NAGATA, Y. (1992) Involvement of D-amino acid oxidase in elimination of D-serine in mouse brain. *Experientia* **48**, 753–755.

NAGATA, Y., HORIIKE, K. & MAEDA, T. (1994) Distribution of free D-serine in vertebrate brains. *Brain Research* **634**, 291–295.

PAXINOS, G. & WATSON, C. (1986) *The Rat Brain in Stereotaxic Coordinates*, 2nd ed. San Diego: Academic Press.

PEROTTI, M.E., GAVAZZI, E., TRUSSRDO, L., MALGARETTI, N. & CURTI, B. (1987) Immunoelectron microscopic localization of D-amino acid oxidase in rat kidney and liver. *Histochemical Journal* **19**, 157–169.

RONCHI, S., MINCHIOTTI, L., GALLIANO, M., CURTI, B., SWENSON, R. P., WILLIAMS, C. H. &

MASSEY, V. (1982) The primary structure of D-amino acid oxidase from pig kidney. *Journal of Biological Chemistry* **257**, 8824–8834.

SCHELL, M. J., MOLLIVER, M. E. & SNYDER, S. H. (1995) D-serine, an endogenous synaptic modulator: localization to astrocytes and glutamate-stimulated release. *Proceedings of the National Academy of Sciences USA* **92**, 3948–3952.

TOWBIN, H., STAHELIN, T. & GORDON., J. (1979) Electrophoretic transfer of proteins from polyacrylamide gels to nitrocellulose sheets: procedure and some applications. *Proceedings of the National Academy of Sciences USA* **76**, 4350–4354.

USUDA, N., YOKOTA, S., HASHIMOTO, T. & NAGATA, T. (1986) Immunocytochemical localization of D-amino acid oxidase in the central clear matrix of rat kidney peroxisomes. *Journal of Histochemistry and Cytochemistry* **34**, 1709–1718.

USUDA, N., YOKOTA, S., ICHIKAWA, R., HASHIMOTO, T. & NAGATA, T. (1991) Immunoelectron microscopic study of a new D-aminoacid oxidase-immunoreactive subcompartment in rat liver peroxisomes. *Journal of Histochemistry and Cytochemistry* **39**, 95–102.

VAN DEN BOSCH, H., SCHUTGENS, R. B. H., WANDERS, R. J. A. & TAGER, J. M. (1992) Biochemistry of peroxisomes. *Annual Reviews in Biochemistry* **61**, 157–197.

VAN ROERMUND, C. W. T., VAN DEN BERG, M. & WANDERS, R. J. A. (1995) Localization of 3-oxoacyl-CoA thiolase in particles of varied density in rat liver: implications for peroxisome biogenesis. *Biochimica et Biophysica Acta* **1245**, 348–358.

WEIMAR, W. R. & NEIMS, A. H. (1977) Hog cerebellar D-amino acid oxidase and its histochemical and immunofluorescence localization. *Journal of Neurochemistry* **28**, 559–572.

ZAAR, K. (1992) Structure and function of peroxisomes in the mammalian kidney. *European Journal of Cell Biology* **59**, 233–254.